FEBS Letters 583 (2009) 1859–1866

FEBS Letters

journal homepage: www.FEBSLetters.org

Transcriptomic and proteomic approach to studying SNX-2112-induced K562 cells apoptosis and anti-leukemia activity in K562-NOD/SCID mice

Lin Jin [a,b,1], Chuan-Le Xiao [c,1], Chun-Hua Lu [c], Min Xia [d], Guo-Wen Xing [e], Sheng Xiong [a], Qiu-Ying Liu [a], Hui Liu [a,b], Yi-Cheng Li [a], Feng Ge [c], Qing-Duan Wang [f], Qing-Yu He [c], Yi-Fei Wang [a,*]

[a] *Guangzhoujinan Biomedicine Research and Development Center, National Engineering Research Center of Genetic Medicine, Jinan University, No.601, West Huangpu Road, Guangzhou 510632 China*
[b] *Institute of Pharmacology Science, Jinan University, Guangzhou 510632, China*
[c] *Institute of Life and Health Engineering, Jinan University, Guangzhou 510632, China*
[d] *Beijing Guoyaolongli Biomedicine New Technology Co. Ltd., Beijing 102600, China*
[e] *Chemistry College, Beijing Normal University, Beijing 100875, China*
[f] *Henan Academy of Medical and Pharmaceutical Sciences, Zhengzhou 450052, China*

ARTICLE INFO

Article history:
Received 21 March 2009
Revised 17 April 2009
Accepted 23 April 2009
Available online 8 May 2009

Edited by Giulio Superti-Furga

Keywords:
SNX-2112
K562 cell
Apoptosis
Transcriptomic
Proteomic
Mitochondria dysfunction

ABSTRACT

SNX-2112, a novel inhibitor of Hsp90 currently used as an anti-tumor drug, induces apoptosis in multiple tumor cell lines. It destabilizes specific client proteins, but the molecular mechanism of the apoptosis effect of SNX-2112 is poorly understood. Here, we analyzed the apoptotic effect of SNX-2112 on human chronic myeloid leukemia (CML) K562 cells. Transcriptomic and proteomic approaches further revealed that caspase signals originated from mitochondria dysfunction, mediated by Akt signaling pathway inactivity. Additionally, SNX-2112 prolonged the survival time of NOD/SCID mice inoculated with K562 tumor cells. Our results demonstrated the therapeutic potential of SNX-2112 against human CML.

Structured summary:
MINT-7033976: *BAD* (uniprotkb:Q92934) *physically interacts* (MI:0218) with *Bcl2-Xl* (uniprotkb:Q07817) by *anti bait coimmunoprecipitation* (MI:0006)

1. Introduction

Hsp90 (heat shock protein 90) is a molecular chaperone that modulates the stability and/or transport of a diverse set of critical cellular regulatory, metabolism, organization, and signaling proteins [1]. It allows cancer cells to tolerate the many components of dysregulated pathways in a transformation specific manner by interacting with several client substrates, such as kinases, hormone receptors and transcription factors directly involved in driving multi-step malignancy, and also with mutated oncogenic proteins required for the transformed phenotype [2].

SNX-2112, a novel inhibitor of Hsp90, selectively binds to the ATP pocket of Hsp90 and is more pharmacologically effective than 17-(allylamino)-17-demethoxygeldanmycin (17-AAG) [3]. Here, we provide evidence that SNX-2112 can induce apoptosis in human chronic leukemia K562 cells. A series of assays revealed that SNX-2112 not only degraded its client protein Bcr-Abl but also impaired mitochondria function resulting in K562 cells apoptosis. Simultaneously, we found a possible mechanism related to Akt signaling pathway inactivity. Furthermore, consecutive injection of SNX-2112 prolonged the survival time of NOD/SCID mice inoculated with K562 cells.

2. Materials and methods

2.1. Reagents, antibodies and cells

SNX-2112 was made by our lab as described [4] with a purity > 98.0%. 17-AAG was from Alexis Biochemicals (San Diego,

Abbreviations: 17-AAG, 17-(allylamino)-17-demethoxygeldanmycin; DMSO, dimethylsulfoxide; CML, chronic myeloid leukemia; FBS, fetal bovine serum; IEF, isoelectric focusing; IPG, immobilized pH gradient; PRDX5, peroxiredoxin V; DLD, dihydrolipoamide dehydrogenase; ECH1, enoyl coenzyme A hydratase 1; IDH3A, isocitrate dehydrogenase alpha subunit; ALDH2, aldehyde dehydrogenase 2 family; NDUFV2, NADH dehydrogenase flavoprotein 2; TRAP1, tumor necrosis factor-associated protein 1; Crkl, v-crk sarcoma virus CT10 oncogene homolog (avian)-like; Grb2, growth factor receptor bound protein 2

* Corresponding author. Fax: +86 20 85223426.
E-mail address: twang-yf@163.com (Y.-F. Wang).

[1] These authors contributed equally to this manuscript.

0014-5793/$36.00 © 2009 Federation of European Biochemical Societies. Published by Elsevier B.V. All rights reserved.
doi:10.1016/j.febslet.2009.04.046

CA). SNX-2112 and 17-AAG stocks at 10 mmol/L dimethylsulfoxide (DMSO) in solution were stored at 4 °C and −20 °C, respectively. Antibodies against these proteins were purchased: caspase-3, 8, 9, PARP, p-Bad (Ser112), and Bcr-Abl protein (Cell Signaling, Beverly, MA); cytochrome *c*, p-Akt(Thr308), Akt, Bad, Bcl-xL,14-3-3 (Epitomics, Burlingame, CA); Crkl, Grb2 and β-actin (Santa Cruz, Santa Cruz, CA). Human chronic myeloid leukemia (CML) K562 cells (ATCC, Manassas, VA) were grown in RPMI-1640 with 10% heat inactivated fetal bovine serum (FBS), and 100 U/ml of penicillin and streptomycin.

2.2. MTT assay

2×10^5 K562 cells were seeded in a 96-well plate with various concentrations of SNX-2112 for 72 h.

Then 20 μl of RPMI-1640 with 10% FBS and 5 mg/ml MTT were added. The precipitated formazan was dissolved in 100 μl of DMSO. Cell viability was assessed at optical density = 570 nm.

2.3. Assessment of apoptosis

Cells were washed in PBS and resuspended in 100 μl of incubation buffer containing Annexin V-FITC and PI. Samples were incubated at RT for 10 min and analyzed by FACS.

2.4. Western blot

Cells were lysed in RIPA buffer and protein measured by Bradford assay. Cell extracts were run on SDS–PAGE, blotted on PVDF membranes, blocked with 5% non-fat milk, and probed with various antibodies. Specific protein bands were visualized with ECL chemiluminescence (Pierce, Rockford, IL) and imaged by autoradiography.

2.5. Transcriptomic analysis

cRNA was prepared and hybridized to Affymetrix Human Genome U133 Plus 2.0 Array. Each microarray dataset was normalized by Robust Multichip Averaging (RMA) method and correlation of all signals intensity > 95%. Triplicate arrays were analyzed with Welch *t*-test. Genes with $P < 0.01$ and a group mean difference $\geqslant 1$ or $\leqslant -1$ were considered significantly modulated and chosen for analysis. Gene Ontology annotation terms were generated with Pathway Studio version 5.0 software (Ariadne Genomis, Rockville, MD). The Kyoto Encyclopedia of ResNet Mammalian database was used as a search tool [5].

2.6. Proteomics analysis

Cells induced with 1 μM SNX-2112 for indicated time were harvested, rinsed, lysed for 30 min at 4 °C, then centrifuged (12 000×*g*, 4 °C) for 15 min. Proteins in the lysates were measured by the Bradford assay, then separated by isoelectric focusing (IEF) using immobilized pH gradient (IPG) drystrips with pH range 3–10 on Ettan IPGphor 3 (General Electric Company, USA) with a voltage gradient. Proteins were resolved in the 2nd dimension with SDS–PAGE and 12.5% gels were stained with silver nitrate overnight. Gel images were analyzed with Image Master 2D Platium 6.0. Peptide mass spectra were obtained on an Applied Biosystem Sciex 4800 MALDI TOF/TOF mass spectrometer.

Data were acquired in a positive MS reflector using a CalMix5 standard for calibration (ABI4700 Calibration Mixture). The MS and MS/MS spectra for each spot were combined and run on the MASCOT search engine (V2.1, Matrix Science, UK) using GPS Explorer software (V3.6, Applied Biosystems). MASCOT protein scores > 61 were statistically significant ($P < 0.05$).

2.7. Isolation of the cytosolic fraction

Isolation of the cytosolic fraction was performed at 4 °C as described [6]. Briefly, cells were lysed in ice-cold sucrose buffer. The lysate was centrifuged at 600×*g* for 10 min to remove nuclei and unbroken cells. Then, supernatant was spun at 14 000×*g* for 15 min to eliminate mitochondria. The supernatant was centrifuged again at 100 000×*g* for 1 h. The protein concentration of the supernatant, representing the cytosolic fraction, was assayed by the Bradford assay. Cytochrome *c* in the cytosolic fraction was then analyzed by Western blot.

2.8. JC-1 for mitochondrial transmembrane potential study

5×10^5 cells were incubated with 10 μg/ml JC-1 for 30 min at 37 °C, then washed with PBS and resuspended in 250 μl PBS. Highly negative membrane potential in mitochondria produces JC-1 red fluorescence. Loss of mitochondrial transmembrane potential results in green fluorescence and loss of the red fluorescence.

2.9. Co-immunoprecipitation (co-IP)

Cells seeded for indicated time were lysed with IP buffer. Clarified cell lysates were incubated with antibodies against specific proteins for 90 min at 4 °C with gentle shaking, then absorbed to protein G plus-agarose beads (Santa Cruz, Santa Cruz, CA). Beads were extensively washed; the eluted complex was resuspended in SDS sample buffer, and separated by 12.5% SDS–PAGE.

2.10. Surface antigen CD13 and CD33 analysis by flow cytometry

Cells were suspended in PBS, stained for 30 min on ice with anti-CD13-PE or CD33-PE and anti-glycophorin A-FITC antibodies (Beckman Coulter, USA). FITC- or PE-labeled mouse IgG alone were negative controls.

2.11. Animals and administration of SNX-2112

Six-eight weeks old NOD/SCID mice from Chinese Academy of Medical Sciences (Beijing, China) were given commercial food, water ad libitum, and housed at 23 ± 5 °C and 55 ± 5% RH through the experiment. Eight mice per group were inoculated by tail vein with 10^7 K562 cells. SNX-2112 was dissolved in saline with 10% DMSO; 17-AAG was dissolved in saline with 10% DMSO including 0.05% Tween-20 [7].

2.12. Statistical analysis

Data were evaluated by Welch *t*-test when only 2 value sets were compared. One-way ANOVA followed by Dunnett's test for 3 or more groups. Survival was analyzed using the Kaplan–Meier log-rank test. Results are expressed as mean ± S.D. with significance at $P < 0.05$ or $P < 0.01$.

3. Results and discussion

3.1. SNX-2112 induced apoptosis in human chronic leukemia K562 cells

We first determined the cytotoxic concentration of SNX-2112 on K562 cells using MTT assays on cells treated with various concentrations of the drug for 72 h. SNX-2112 showed a dose-dependent cytotoxic effect with IC50 = 0.92 μM (Fig. 1A). Then, we evaluated the apoptotic effect by flow cytometry of Annexin V-FITC

and PI labeled K562 cells treated with SNX-2112 or 17-AAG as the positive control. The ratio of apoptotic cells increased from 10.6 ± 2.1% up to 75.8 ± 7.4% after exposure to SNX-2112 at 0.05–10 μM, significantly greater than with 17-AAG (Fig. 1B).

We next analyzed the effect of SNX-2112 on cleavage of caspase family proteins to determine whether caspase activation contributes to SNX-2112-induced K562 cell apoptosis. The activation of caspase-3, the major effector caspase, requires activation of initiator caspases such as caspase-8 or -9 in response to pro-apoptotic signaling [8]. The cleavage of PARP is a specific hallmark of activated caspase-3 [9,10]. Notably, we observed a substantial increase in caspase-9 activity with SNX-2112 from 1 to 10 μM (Fig. 1C, upper). Treatment with 0.1 and 0.05 μM of the agent, respectively, also did not induce complete cleavage of caspase-9, indicating early apoptosis in the cells. SNX-2112 also dose-dependently induced pro-caspase-3 degradation (Fig. 1C, middle) which could lead to caspase-3 activation. Intracellular pro-PARP also dose-dependently decreased with a corresponding increase in cleavage of the 116 to 89-kDa protein (Fig. 1C, bottom). At low dose of 0.1 μM, SNX-2112 did not activate pro-caspase-3 and PARP. Caspase-8 is an upstream caspase that relays the death signal from Fas receptor–ligand interactions to the downstream caspase-3 and processes pro-caspase-3 [11]. However, pro-caspase-8 was not cleaved and its total level was unchanged (Fig. 1C), indicating the FasL/Fas pathway may not be involved in SNX-2112 induced apoptosis.

Therefore, SNX-2112 activated initiator caspase-9, which is closely coupled to pro-apoptotic signals. Once activated, caspase-9 activated downstream effector caspase-3, which in turn cleaved nuclear protein PARP. Based on these results, the treatment condition with SNX-2112 at 1 μM was selected for the following analysis.

3.2. Apoptosis induced by SNX-2112 is related to mitochondria dysfunction

The findings above indicated that SNX-2112 may trigger the intrinsic mitochondrial pathway of apoptosis. In addition to energy production, mitochondria are involved in many cellular processes such as metabolism, signaling, cell growth and apoptosis [12,13]. Mitochondrial dysfunctions and cytochrome *c* release to the cytosol are significantly associated with caspase activation [14]. To provide molecular evidence for mitochondrial dysfunction in response to SNX-2112, we comprehensively profiled alterations in gene expression upon treatment. Prepared RNA from K562 cells treated with or without 1 μM SNX-2112 for 48 h were hybridized to Affymetrix Human Genome U133 Plus 2.0 Array chips. Randomly selected genes from the microarray results were confirmed by real-time PCR (data not shown). In all, 229 genes accounting for 10.75% of total selectors were up-regulated or down-regulated compared with control group. Among these, 136 and 93 genes have known and unknown functions, respectively (Supplementary Tables 1 and 2). Of the 136 known genes classified according to various functional groups (Fig. 2A), 62.51% were related to various metabolism groups and up- or down-regulated to different degrees, suggesting mitochondria dysfunction [15]. Except for coenzyme and prosthetic group, numerous genes related to different substance metabolism groups tended to down-regulate (Fig. 2B), indicating that the defect in mitochondrial function can directly inhibit genes encoding metabolism [16]. We attributed the few up-regulated genes (Fig. 2B) to the dysfunction feedback signal, which may trigger new compensatory metabolism gene synthesis.

We also found 7 proteins involved in mitochondrial dysfunction from 55 identified proteins by proteomics analysis (Table 1). Peroxiredoxin V (PRDX5) is an antioxidant enzyme which neutralize reactive oxygen species (ROS). Here, PRDX5 protein levels consistently increased from 48 to 72 h, indicating that ROS produced by mitochondria can stimulate high levels of PRDX5 to further protect mitochondrial from impairment [17,18]. Over-expression of dihydrolipoamide dehydrogenase (DLD), a pro-oxidant, can lead to high ROS that induces mitochondrial damage [19,20]. In our study, up-regulated DLD expression also provided indirect evidence for mitochondrial dysfunction. Enoyl coenzyme A hydratase 1 (ECH1) was up-regulated > 2-fold, suggesting that high expression of ECH1 in mitochondria may stimulate the degradation of medium-chain and short-chain, further disturbing fatty acid normal metabolism [21]. The human mitochondrial NAD(+)-specific isocitrate dehydrogenase alpha subunit (IDH3A) is a NAD(+)-dependent isocitrate dehydrogenase, catalyzing the regulated rate-limiting step of the tricarboxylic acid cycle where the bulk of ATP maintaining homeostasis is produced. Decrease of IDH3A protein contributes to the reduction of ATP and down-regulation of energy metabolism in mitochondria. We also found 2 down-regulated proteins involved in the mitochondrial electron transport: aldehyde dehydrogenase 2 family (ALDH2) and NADH dehydrogenase flavoprotein 2 (NDUFV2). Additionally, the NDUFV2 protein dot reduced dramatically after treatment with SNX-2112 for 48 h. Reduced proteins participating in respiratory chain transport can directly impair the electron transport in the mitochondrial inner membrane. The latter can increase ROS and induce apoptosis [22]. Finally, the tumor necrosis factor-associated protein 1 (TRAP1) also decreased >2 fold in our 2-D analysis. TRAP1 is a mitochondrial heat shock protein, which can help its client proteins fold correctly in mitochondria. Its high protein levels interfere with caspase-3 activation and protect cells from oxidative stress [23]. Our results confirmed the above conclusion and indicated that TRAP1 may be an indirect effector target of SNX-2112. In addition, except DLD and ALDH2, the expression of the other 5 proteins corresponded to the changes on mRNA transcript expression.

In mitochondria, cytochrome *c* is required as an electron carrier during oxidative phosphorylation. The electron transport mediated by cytochrome *c* generates a proton gradient across the inner mitochondrial membrane required to maintain potential $\Delta\Psi$. Thus, the release of cytochrome *c* from the electron transport chain is expected to impair the electron flow and cause a decrease in $\Delta\Psi$. Simultaneously, cytochrome *c* is released into the cytosol and activates pro-caspase-9 by binding apaf-1 [24,25]. Here, SNX-2112 (1 μM) induced the time-dependent release of mitochondrial cytochrome *c* into the cytosol of K562 cells (Fig. 2C). Compared to untreated control, cytochrome *c* was visible at 12 h and fully developed at 24 h. Furthermore, we used the potential sensitive dyes JC-1 to study the mitochondrial $\Delta\Psi$. After SNX-2112 treatment for 24 h, $\Delta\Psi$ decreased in a time-dependent manner, demonstrating a disruption of the $\Delta\Psi$ during K562 apoptosis (Fig. 2D).

3.3. SNX-2112 caused Bad activation and the association of Bad and Bcl-xL mediated by Akt signaling pathway

We thus studied transduction signals leading to mitochondria dysfunction using a global proteomics approach to identify v-crk sarcoma virus CT10 oncogene homolog (avian)-like (Crkl) and growth factor receptor bound protein 2 (Grb2), 2 common upstream cell signaling proteins. Both Crkl and Grb2 proteins were reduced in Western blots after 48 h of SNX-2112 treatment, in agreement with spot intensities from the 2-DE gels (Fig. 3A). Crkl and Grb2 are known as adaptor proteins in p210Bcr-Abl complexes also including Bcr-Abl itself [26,27], one of Hsp90 clients that can be degraded by Hsp90 inhibitor [28,29]. Here, we found SNX-2112 could lower expression of Bcr-Abl to almost undetectable levels (Fig. 3B). We speculate that SNX-2112 led to degradation of Bcr-Abl and decomposition of p210Bcr-Abl complexes to further down-regulate levels of Crkl and Grb2. Currently, we are investigating the underlying mechanisms.

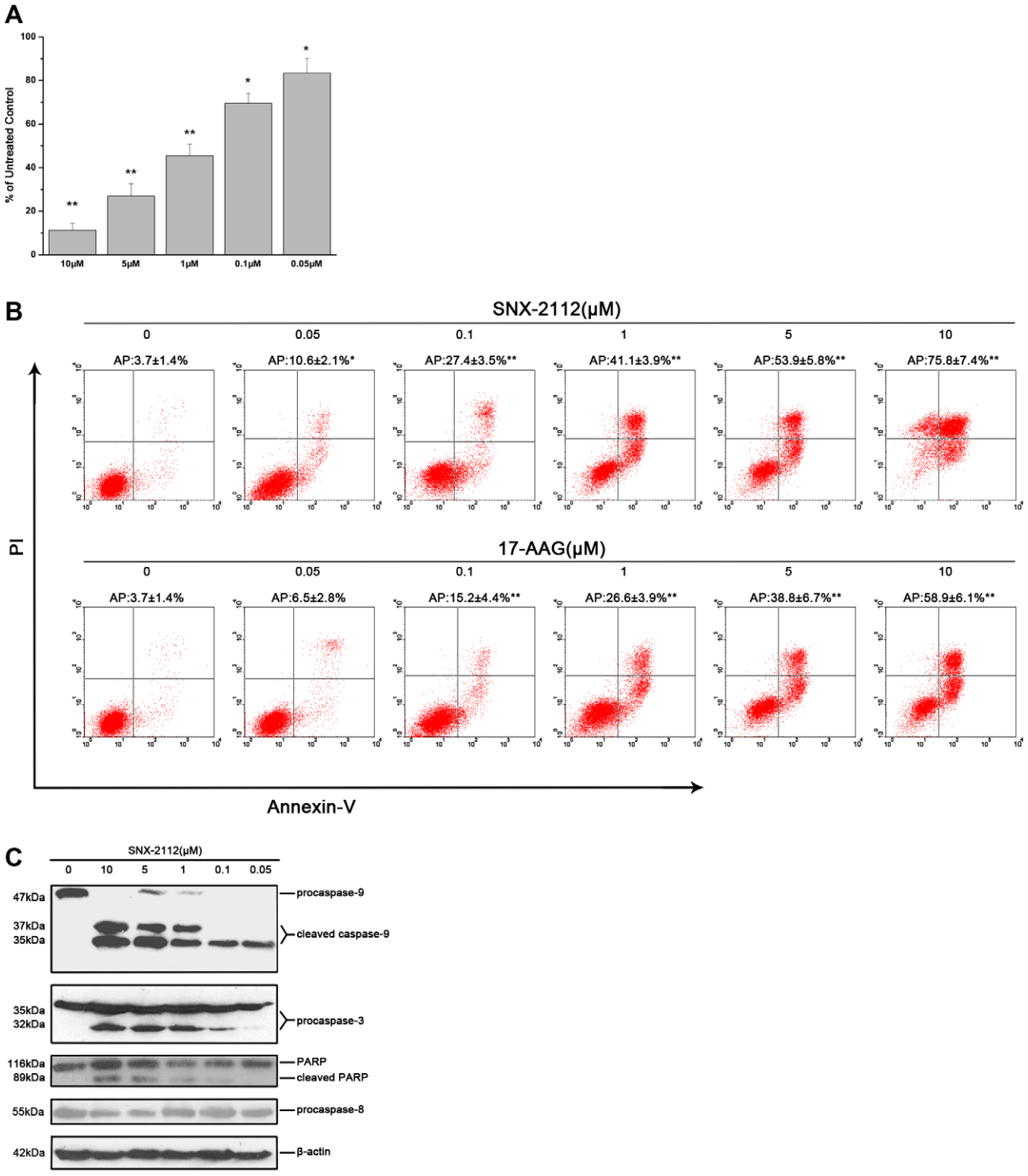

Fig. 1. SNX-2112 induced apoptosis in K562 cells. (A) MTT assay of cytotoxicity in K562 cells cultured for 72 h with various doses of SNX-2112. Data are means ± S.D. of 3 repeats. $^{*}P < 0.05$ and $^{**}P < 0.01$, compared to untreated control. (B) Evaluation of apoptosis by Annexin V-FITC and PI binding assay after SNX-2112 treatment. $n = 3$ independent experiments. Data are means ± S.D. of 3 repeats. $^{*}P < 0.05$ and $^{**}P < 0.01$, compared to untreated control. (C) SNX-2112 effect on apoptosis-related proteins expression. Fifty micrograms of whole-cell lysate of K562 cells treated with indicated concentration for 72 h for detection of pro-caspase-3, 8, 9 and PARP by Western blot. β-Actin was a loading control. $n = 3$ independent experiments.

Crkl and Grb2 are signal molecules that participate together in Akt signaling transduction [30,31]. As expected, 1 μM SNX-2112 caused significant Akt dephosphorylation after 12 h of treatment (Fig. 3C), while the Akt protein level was not affected by SNX-2112. Additionally, our results suggested Akt signaling was much more rapid compared to Crkl and Grb2 reduction, which partly due to Bcr-Abl kinase degradation lead to the two adaptor proteins inactivate the function such as SH2 and SH3 domains binding Akt substrate and reduce phosphorylation of its target Akt, finally the dysfunction effect served as a feed-back resulted in their self-down-regulation [26,32]. Then, co-IP and Western blots were used to analyze the interaction between Bcl-xL and Bad whose phos-

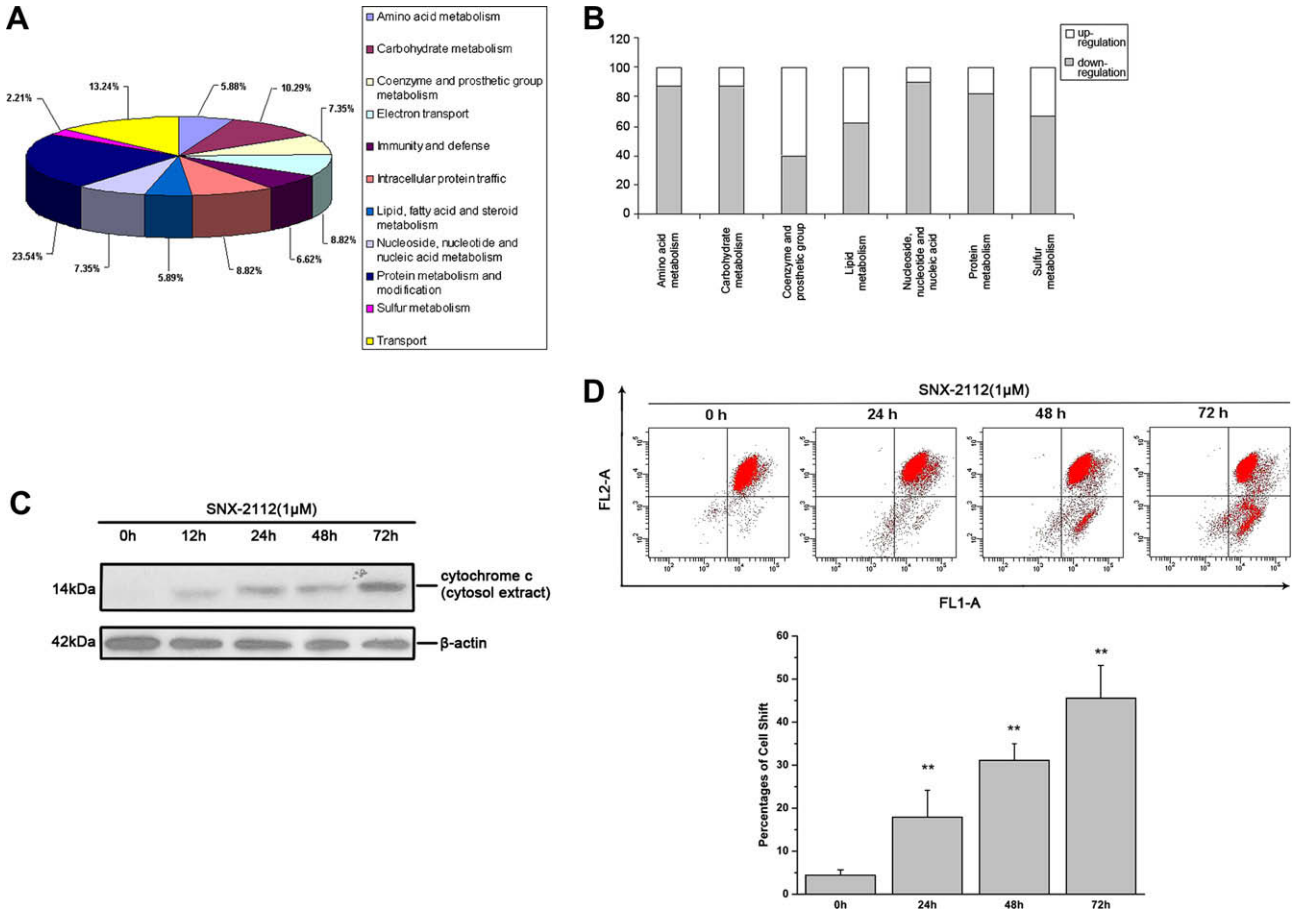

Fig. 2. Mitochondria dysfunction analyzed by a series of assays. (A) Functional classification of mitochondrial genes from SNX-2112 treated K562 cells. (B) Percentage summary of changes on the functional genes grouping related to mitochondrial metabolism. (C) Western blot of cytochrome *c* release in cytosol with treatment of K562 cells with 1 μM SNX-2112. β-Actin was a loading control. Experiment repeated 3 times. (D) Representative flow cytometric analyses of mitochondrial membrane potential using JC-1. The shift of JC-1 fluorescence from orange (FL2-A) to green (FL1-A) indicates a collapse of mitochondrial membrane potential. The % of cells with low mitochondrial membrane potential was measured. Values are mean ± S.D. of 3 repeats. $^{**}P < 0.01$, compared to untreated group.

phorylation is controlled by Akt pathway [33]. Here, phosphorylation of Bad was significantly down-regulated after 12 h of SNX-2112 treatment while total Bad protein levels did not change (Fig. 3D). Moreover, SNX-2112 induced the dissociation of Bad from 14-3-3 and more Bcl-xL was observed to interact with Bad, accordingly (Fig. 3D).

3.4. SNX-2112 effect on survival time of NOD/SCID mice inoculated with K562 cells

Finally, we tested the effect of SNX-2112 on survival of NOD/SCID mice inoculated with K562 cells. The mice were given 10^7 K562 cells in the tail vein to mimic human chronic leukemia invasion [34]. Three randomized groups included: SNX-2112, 17-AAG and control. We analyzed the expression of 2 significant surface antigens, $CD13^+$ and $CD33^+$, on myeloid leukemia K562 by FACS. On day 5, >1% $CD13^+$ and >1.5% $CD33^+$ were detected in mice peripheral blood, indicating that numerous human K562 cells had engrafted and proliferated in the mice. The mice were then treated with 6 mg/kg SNX-2112 by tail vain injection from days 5–9 and days 12–16. At the same time, 12 mg/kg 17-AAG was injected IP into another group. Untreated mice inoculated with K562 cells died of diffuse leukemia while there was obvious lower expression of $CD13^+$ and $CD33^+$ in SNX-2112 group vs. control group (Fig. 4A). Sur-

Table 1
Up- and down-regulated proteins related with mitochondrial function identified by proteomics analysis.

Protein name	Accession number	Sequence coverage (%)	PI/Mr (Da)	Fold change		Function
				48 h	72 h	
PRDX5	IPI00759663	11	6.73/17020	12.7↑	10.9↑	Oxidoreductase activity
ECH1	IPI00011416	26	8.16/35793	2.1↑	3.3↑	Fat acid metabolism
DLD	IPI00015911	19	7.59/54116	2.2↑	2.8↑	Oxidoreductase activity
IDH3A	IPI00374151	10	5.84/31361	2.5↓	3.1↓	Carbohydrate metabolic process
TRAP1	IPI00030275	23	7.21/57184	2.6↓	2.1↓	Mitochondrial HSP90 protein against apoptosis
ALDH2	IPI00216805	48	5.79/56688	2.2↓	2.4↓	Mitochondrial electron transport
NDUFV2	IPI00291328	15	8.22/27374	>100↓		Mitochondrial electron transport

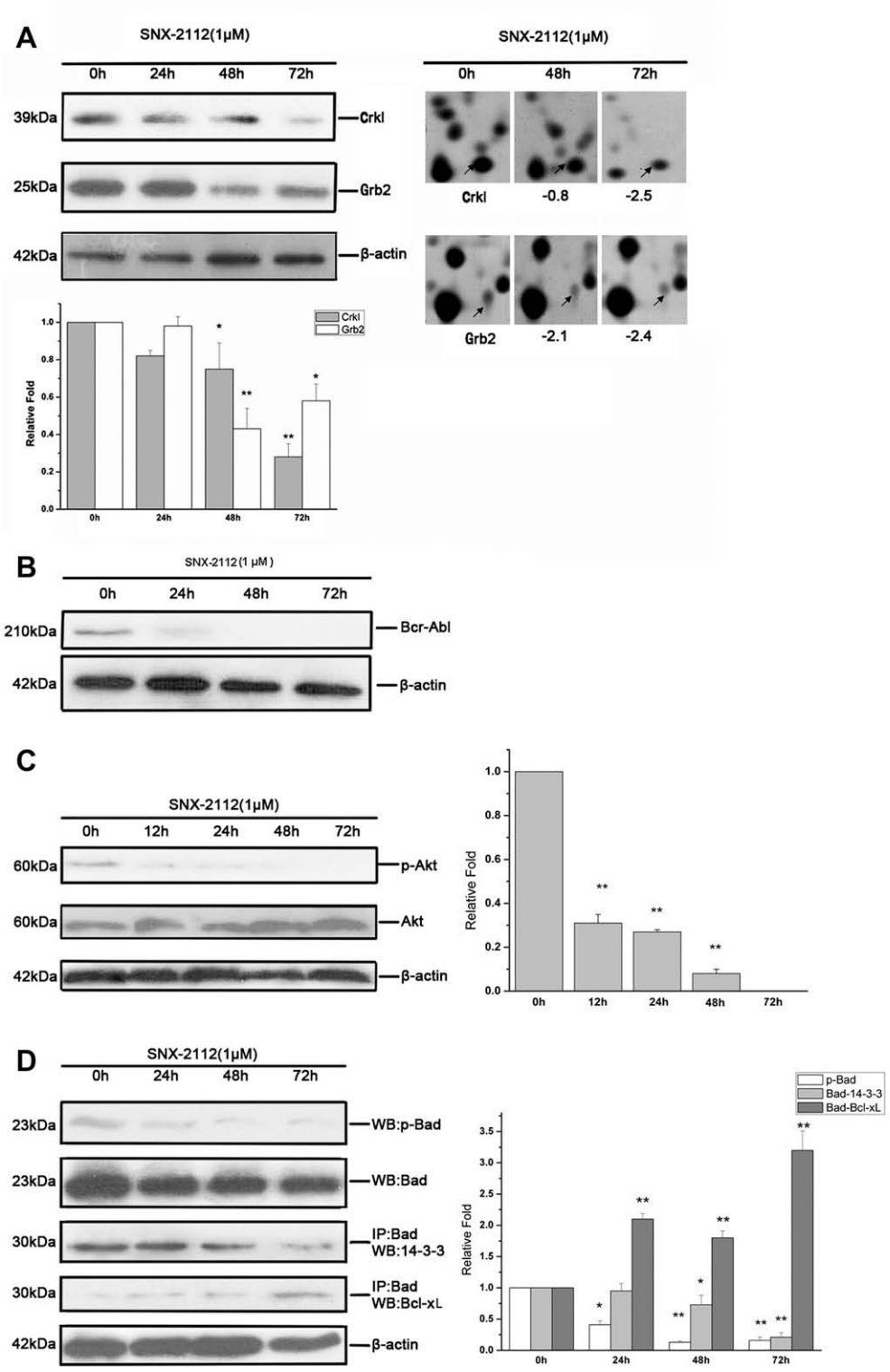

Fig. 3. SNX-2112 caused Bad activation and the association of Bad and Bcl-xL mediated by Akt signaling pathway. (A) Crkl and Grb2 protein analysis after SNX-2112 treatment of cells for indicated time. *Left*, Western blot detecting Crkl and Grb2 protein and normalized on bar graph with β-actin. Results are mean ± S.D. of 3 repeats. *Right*, Detailed alterations of Crkl and Grb2 identified by 2-DE. (B) Western blot of Bcr-Abl protein of cells treated with of 1 μM SNX-2112. Experiment repeated 3 times. (C) Expression of phosph-Akt and Akt in induced cells from 0 to 72 h, and normalized by β-actin in bar graph. Results are mean ± S.D. of 3 repeats. (D) Co-IP and Western blot were used to test interactions between Bad and Bcl-xL in apoptosis. Cell lysates were incubated with anti-Bad antibody. β-Actin was a loading control. The histogram represents 3 separate experiments. $^{*}P < 0.05$ and $^{**}P < 0.01$, compared with untreated cells.

vival time of all SNX-2112 treated mice was longer than that of untreated mice ($P < 0.01$), ranging 47 to >80 days (Fig. 4B). Untreated mice had the shortest survival time of 30–53 days. Survival time of 17-AAG treated mice was from 39 to 66 days.

In conclusion, SNX-2112, a novel Hsp90 inhibitor, depleted Bcr-Abl client protein and induced apoptosis in human CML cells though mitochondria dysfunction mediated by Akt signaling pathway. SNX-2112 clearly has anti-K562 activity in the small animal

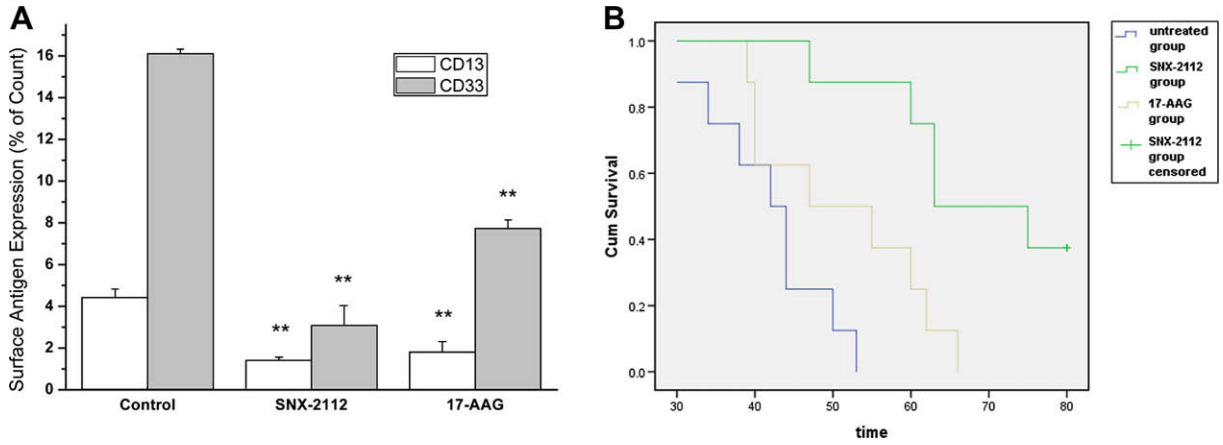

Fig. 4. SNX-2112 showed therapeutic effect on NOD/SCID mice inoculated with K562 cells. (A) CD13 and CD33 surface antigen analysis by flow cytometry. The histogram represents at least 3 separate experiments. $^{**}P < 0.01$, compared to untreated cell. (B) SNX-2112 treatment prolonged survival of NOD/SCID mice inoculated with K562 cells. Survival study was analyzed with the Kaplan–Meier log-rank test.

model, suggesting this agent may have therapeutic potential against CML.

Acknowledgments

This work was supported by Grants from the Nation "863" Program of China (No. 2007AA02Z142), the Nation "211 project" and the National Natural Science Foundation of China (No. 30873082).

Appendix A. Supplementary data

Supplementary data associated with this article can be found, in the online version, at doi:10.1016/j.febslet.2009.04.046.

References

[1] Maloney, A. and Workman, P. (2002) Hsp90 as a new therapeutic target for cancer therapy: the story unfolds. Exp. Opin. Biol. Ther. 2, 3–24.
[2] Ruden, D.M., Xiao, L., Garfinkel, M.D. and Lu, X. (2005) Hsp90 and environmental impacts on epigenetic states: a model for the trans-generational effects of diethylstibesterol on uterine development and cancer. Hum. Mol. Genet. 14, 149–155.
[3] Chandarlapaty, S. et al. (2008) SNX2112, a synthetic heat shock protein 90 inhibitor, has potent antitumor activity against HER kinase-dependent cancers. Clin. Cancer Res. 14, 240–248.
[4] Barta, T.E. et al. (2008) Discovery of benzamide tetrahydro-4H-carbazol-4-ones as novel small molecule inhibitors of Hsp90. Bioorg. Med. Chem. Lett. 18, 3517–3521.
[5] Nikitin, A., Egorov, S., Daraselia, N. and Mazo, I. (2003) Pathway studio the analysis and navigation of molecular networks. Bioinformatics 19, 2155–2157.
[6] Pastorino, J.G., Tafani, M. and Farber, J.L. (1999) Tumor necrosis factor induces phosphorylation and translocation of BAD through a phosphatidylinositide-3-OH kinase-dependent pathway. J. Biol. Chem. 274, 19411–19416.
[7] Kelland, L.R., Sharp, S.Y., Rogers, P.M., Myers, T.G. and Workman, P. (1999) DT-Diaphorase expression and tumor cell sensitivity to 17-allylamino, 17-demethoxygeldanamycin, an inhibitor of heat protein 90. J. Natl. Cancer Inst. 91, 1940–1949.
[8] Nicholson, D.W. et al. (1995) Identification and inhibition of the ICE/CED-3 protease necessary for mammalian apoptosis. Nature 376, 3–43.
[9] Cohen, G.M. (1997) Caspases: the executioners of apoptosis. Biochem. J. 326, 1–16.
[10] Nagata, S. (1997) Apoptosis by death factor. Cell 88, 355–365.
[11] Budihardjo, I., Oliver, H., Lutter, M., Luo, X. and Wang, X. (1999) Biochemical pathways of caspase activation during apoptosis. Annu. Rev. Cell Dev. Biol. 15, 269–290.
[12] Wallace, D.C. (2005) A mitochondrial paradigm of metabolic and degenerative diseases, aging, and cancer: a dawn for evolutionary medicine. Annu. Rev. Genet. 39, 359–407.
[13] Tang, T., Zheng, B., Chen, S.H., Murphy, A.N., Kudlicka, K., Zhou, H.L. and Farquhar, M.G. (2009) HNOA1 interacts with complex I and DAP3 and regulates mitochondrial respiration and apoptosis. J. Biol. Chem. 284, 5414–5424.
[14] Sánchez-Alcázar, J.A., Khodjakov, A. and Schneider, E. (2001) Anticancer drugs induce increased mitochondrial cytochrome *c* expression that precedes cell death. Cancer Res. 61, 1038–1044.
[15] Cimini, D., Patil, K.R., Schiraldi, C. and Nielsen, J. (2009) Global transcriptional response of Saccharomyces cerevisiae to the deletion of SDH3. BMC Syst. Biol. 3, 17.
[16] Hansson, A., Hance, N., Dufour, E., Rantanen, A., Hultenby, K., Clayton, D.A., Wibom, R. and Larsson, N.G. (2004) A switch in metabolism precedes increased mitochondrial biogenesis in respiratory chain-deficient mouse hearts. Proc. Natl. Acad. Sci. USA 101, 3136–3141.
[17] Kropotov, A., Usmanova, N., Serikov, V., Zhivotovsky, B. and Tomilin, N. (2007) Mitochondrial targeting of human peroxiredoxin V protein and regulation of PRDX5 gene expression by nuclear transcription factors controlling biogenesis of mitochondria. FEBS J. 274, 5804–5814.
[18] Banmeyer, I., Marchand, C., Clippe, A. and Knoops, B. (2005) Human mitochondrial peroxiredoxin 5 protects from mitochondrial DNA damages induced by hydrogen peroxide. FEBS Lett. 579, 2327–2333.
[19] Petrat, F., Paluch, S., Dogruoz, E., Dorfler, P., Kirsch, M., Korth, H.G., Sustmann, R. and de Groot, H. (2003) Reduction of Fe(III) ions complexed to physiological ligands by lipoyl dehydrogenase and other flavoenzymes in vitro: implications for an enzymatic reduction of Fe(III) ions of the labile iron pool. J. Biol. Chem. 278, 46403–46413.
[20] Sy, L.K., Yan, S.C., Lok, C.N., Man, R.Y. and Che, C.M. (2008) Timosaponin A-III induces autophagy preceding mitochondria-mediated apoptosis in HeLa cancer cells. Cancer Res. 68, 10229–10237.
[21] He, X.Y., Yang, S.Y. and Schulz, H. (1992) Inhibition of enoyl-CoA hydratase by long-chain L-3-hydroxyacyl-CoA and its possible effect on fatty acid. Arch Biochem. Biophys. 298, 527–531.
[22] Pelicano, H., Feng, L., Zhou, Y., Carew, J.S., Hileman, E.O., Plunkett, W., Keating, M.J. and Huang, P. (2003) Inhibition of mitochondrial respiration: a novel strategy to enhance drug-induced apoptosis in human leukemia cells by a reactive oxygen species-mediated mechanism. J. Biol. Chem. 278, 37832–37839.
[23] Montesano, G.N., Chirico, G., Pirozzi, G., Costantino, E., Landriscina, M. and Esposito, F. (2007) Tumor necrosis factor-associated protein 1 (TRAP-1) protects cells from oxidative stress and apoptosis. Stress 10, 342–350.
[24] Hatefi, Y. (1985) The mitochondrial electron transport and oxidative phosphorylation system. Annu. Rev. Biochem. 54, 1015–1069.
[25] Reed, J.C. (1997) Cytochrome *c*: can't live with it – can't live without it. Cell 91, 559–562.
[26] Patel, H., Marley, S.B. and Gordon, M.Y. (2006) Detection in primary chronic myeloid leukaemia cells of p210BCR-ABL1 in complexes with adaptor proteins CBL, CRKL, and GRB2. Genes Chromosomes Cancer 45, 1121–1129.
[27] Sattler, M. et al. (1996) The proto-oncogene product p120CBL and the adaptor proteins CRKL and c-CRK link c-ABL, p190BCR/ABL and p210BCR/ABL to the phosphatidylinositol-3′ kinase pathway. Oncogene 12, 839–846.
[28] Rao, R. et al. (2008) HDAC6 inhibition enhances 17-AAG – mediated abrogation of hsp90 chaperone function in human leukemia cells. Blood 112, 1886–1893.
[29] Barnes, D.J., De, S., van Hensbergen, P., Moravcsik, E. and Melo, J.V. (2007) Different target range and cytotoxic specificity of adaphostin and 17-allylamino-17-demethoxygeldanamycin in imatinib-resistant and sensitive cell lines. Leukemia 21, 421–426.
[30] Park, T.J. and Curran, T. (2008) Crk and Crk-like play essential overlapping roles downstream of disabled-1 in the Reelin pathway. J. Neurosci. 28, 13551–13562.

[31] Dance, M., Montagner, A., Yart, A., Masri, B., Audigier, Y., Perret, B., Salles, J.P. and Raynal, P. (2006) The adaptor protein Gab1 couples the stimulation of vascular endothelial growth factor receptor-2 to the activation of phosphoinositide 3-kinase. J. Biol. Chem. 281, 23285–23295.
[32] Zandy, N.L. and Pendergast, A.M. (2007) Abl tyrosine kinases modulate cadherin-dependent adhesion upstream and downstream of Rho family GTPases. Cell Cycle 7, 444–448.
[33] Datta, S.R., Dudek, H., Tao, X., Masters, S., Fu, H., Gotoh, Y. and Greenberg, M.E. (1997) Akt phosphorylation of BAD couples survival signals to the cell-intrinsic death machinery. Cell 91, 231–241.
[34] Wolff, N.C. and Ilaria Jr., R.L. (2001) Establishment of a murine model for therapy-treated chronic myelogenous leukemia using the tyrosine kinase inhibitor STI571. Blood 98, 2808–2816.